Energy Education Science and Technology Part A: Energy Science and Research
2012 Volume (issues) **30(1):** 55-64

Relationship between deep, maximum and minimum temperatures and their locations in one layer grounds in Turkey

Arif Ozbek[1,*], Tuncay Yilmaz[1], Orhan Buyukalaca[2], Alper Yilmaz[1]

[1] *University of Cukurova, Department of Mechanical Engineering, 01330 Adana, Turkey*
[2] *Osmaniye Korkut Ata University, Faculty of Engineering, Department of Energy Systems Engineering, Osmaniye, Turkey*

Received: 04 September 2011; accepted: 13 November 2011

Abstract

Ground surface temperatures and ground temperatures at different depths are required for the design of Ground-Source Heat Pump (GSHP) systems. The State Meteorological Affairs General Directorate (DMİ) measures the ground temperatures at certain depths at some stations in Turkey. However, these measurements are valid only for the ground structures and properties at the measurement locations and, therefore, can not be used for other ground and ground surface properties. In this study, one layer ground temperatures were calculated numerically using at least 20 years daily mean values of ambient temperature, solar radiation, relative humidity and wind velocity. The data were taken from DMİ for 20 cities selected from different climatic regions in Turkey. The depths for maximum and minimum temperatures in the soil and yearly constant temperatures at 12 m depth from the soil surface (soil end temperatures) were expressed in equations using the numerically calculated temperatures. It was found that soil end temperature is mainly dependent on the yearly mean air temperature. Other parameters that have also influence on the soil end temperature are soil surface absorption coefficient, evaporation fraction and yearly mean solar radiation. Maximum and minimum temperatures are only 0.48 °C higher and lower than the soil end temperature, respectively.

Keywords: One layer ground; Ground temperature distribution; Deep, Maximum and minimum ground temperatures
©Sila Science. All Rights Reserved.

1. Introduction

The need for ground temperature distribution has increased in recent years parallel to the increase in ground source heat pumps (GSHP) applications. The ground temperature is higher than ambient temperature in winter months and vice-versa in summer months and therefore, GSHP's have become attractive. Many numerical and analytical studies were carried out for the determination of ground temperatures.

Analytical models to predict the ground surface and ground temperature distribution were developed. The ground surface temperature variation in the form of sine-wave or Fourier

*Corresponding author. Tel:+90-322-338-6084; fax:+90-322-338-6126.
E-mail address: arozbek@cu.edu.tr (A. Ozbek).

series was assumed [1]. The data obtained from the model with real long-term measurements was compared [2]. Ground surface and ground temperatures for bare or grass covered ground were investigated [3]. Two estimation methods for determining the daily and annual variation of ground surface temperature were presented [4]. A simple model to estimate ground heat flux as a function of ground thermal properties and meteorological data was suggested [5]. A model that can be used to predict monthly ground temperature using monthly meteorological data was developed [6]. Subsurface ground temperature profiles using two different analytical approaches were estimated. In the first one an analytical model was examined based on annual and daily sinusoidal fluctuations of the ground temperature. In the second one, a semi-empirical model was developed using daily average temperatures [7]. A model to estimate daily soil temperature at different depths using meteorological parameters in an arid region was developed [8]. The Artificial Neural Networks (ANN) and Regression Analysis methods were used in estimating monthly average daily global solar radiation arriving on horizontal surface with the help of meteorological and geographic data [9].

Some numerical methods to determine ground temperature were developed. A numerical model of heat conduction to estimate the magnitude of the heat released by freezing during the winter months was used [10]. A model to predict surface temperatures of the different grounds using meteorological data was described [11]. A mathematical model for horizontal type ground heat exchangers was developed [12]. A model that uses meteorological data and some ground parameters as the inputs of the model was presented. The model can be used to estimate ground surface heat fluxes, surface and ground temperature change and other important micrometeorological parameters. The simulated ground temperatures with the micrometeorological measurements were also compared [13]. A two-dimensional numerical simulation of ground-heat transfer adjacent to an experimental earth–contact structure was presented. The numerical and experimental results were compared [14]. A numerical model to estimate the ground temperatures in dry and wet bare grounds was developed [15].

Because temperature distribution in the ground can only be calculated accurately using numerical methods, ground surface temperature and ground temperatures at various depths were determined with a numerical model developed in this work. In the calculations, daily mean values of ambient temperature, solar energy, relative humidity and wind velocity were used for yearly calculations of ground temperature distribution [16-28]. In addition, ground temperatures for 20 cities selected from four different climatic regions in Turkey were calculated. In these cities, measurements are undertaken continuously at least 20 years. In this study saturation pressure of water vapor are determined exactly at each time step using exact correlation between temperature and saturation pressure of water vapor.

The objective of this work is to describe soil end temperature, soil maximum and soil minimum temperatures and the depth of maximum and minimum temperatures, which depend on the climatic data such as yearly mean temperature, yearly mean solar radiation and on the physical properties of the soil such as surface absorption coefficient and thermal diffusivity.

2. Methodology

Heat transfer in one layer homogeneous ground can be written by one dimensional time depended differential equation by assuming constant ground physical properties as follows:

$$\frac{\partial T}{\partial t} = a \frac{\partial^2 T}{\partial x^2} \tag{1}$$

Eq. 1 can be solved writing two boundary conditions at the ground surface and ground depth.

Locations of two boundary conditions for one layer homogeneous ground are shown in Fig. 1.

The following equation can be written at the surface of the ground [1, 3, 4]:

$$x = 0 \quad : \quad -k \left(\frac{\partial T}{\partial x} \right) = h \left(T_a - T_s \right) + a_s \, \dot{q} - \dot{q}_{lw} - \dot{q}_v \tag{2}$$

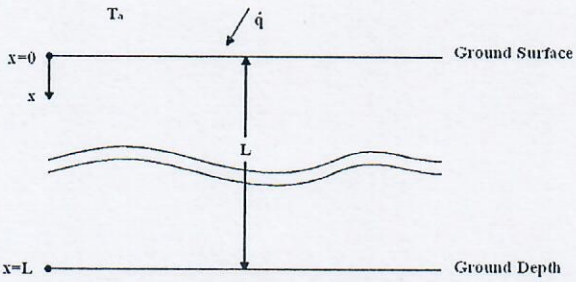


Fig. 1. Locations of two boundary conditions.

Long-wave radiation heat flux ($\dot{q}_{lw}$) can be taken as constant according to [1] and [3]:

$$\dot{q}_{lw} = 63\ W/m^2 \tag{3}$$

For $\dot{q}_v$ the following equation is used [3]:

$$\dot{q}_v = 0.0168\ f\ h(p_{ss} - \varphi\ p_{sa}) \tag{4}$$

For the calculation of P_{ss}, the exact relationship between surface temperature and P_{ss} is used by [16].

For h, the following equation is used by [1]:

$$h = 2.8 + 3u \tag{5}$$

where u is the wind velocity (m/s).

The following equation is valid in the ground depths:

$$x = L \quad : \quad \frac{\partial T}{\partial x} = 0 \tag{6}$$

This condition is satisfied for all soil types, if L is taken as 12 m.

Differential Eq. (1) with the non-linear boundary conditions in Eqs. (2) and (6) was solved iteratively using finite difference method by [16]. Details of numerical methods and temperature distribution were given in the mentioned work. An example of the numerical results for the temperature distribution is given in Fig. 2. In this figure, the maximum, minimum and ground end temperatures are shown.

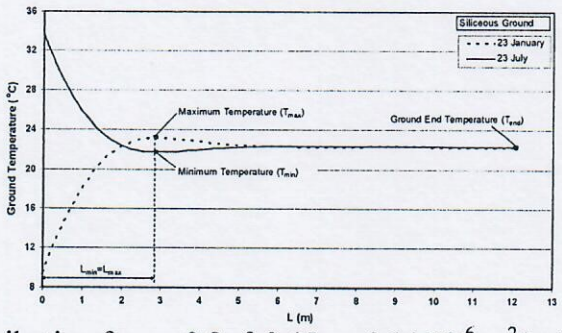


Fig. 2. Temperature distribution for a_s=0.9, f=0.45, a=0.14 10^{-6} m^2/s, k=0.52 W/m°C in Adana for 23 January and 23 July.

3. Results

Ground surface and ground temperatures were calculated for different soil types in this study. Some thermal properties are given for commonly encountered soil types in Table 1.

Ground surface and ground temperatures for the cities in Table 2 were calculated using at least 20 years (between 1985 and 2010) daily mean values of ambient temperature, solar radiation, relative humidity and wind velocity taken from DMI. The depths at which the maximum and the minimum ground temperatures occur and ground end temperatures were determined. Relationships for maximum, minimum and ground end temperatures are given.

It was suggested [1] 0.9 for the value of a_s in Eq. 2, while [20] recommended a value between 0.85 and 0.95.

The value of parameter f depends on ground cover and moisture content of the ground. For bare ground, f can be estimated as follows [1]:

f=1.0 saturated ground
f=0.6-0.8 humid ground
f=0.4-0.5 dry ground
f=0.1-0.2 arid ground

For grass covered grounds, 70% of the above given f values were recommended by [1].

In this study, the analysis was carried out for f=0.45 when a_s was varied between 0.6 to 0.9 and for a_s = 0.9 when f was varied between 0.4 to 0.8.

Table 1. Thermal properties of some soil types

Ground Type	$a.10^6$ [m²/s]	k [W/m°C]
Siliceous ground	0.14	0.52
Dry-heavy ground	0.52	0.95
Humid-heavy ground	0.65	1.30
Granite	1.13	2.93

3. 1. Relationship between ground end and mean temperatures

The temperature difference that was defined using ground end temperature, T_{end} (constant temperature 12 m depth from the ground surface) and the average value of 20 years daily mean ambient temperature (T_{mean}):

$$\Delta T_{end} = T_{end} - T_{mean} \tag{7}$$

was determined using the results obtained from the numerical model.

Variation of ΔT_{end} with absorption coefficient (a_s) and evaporation fraction (f) is discussed below.

Variation of temperature difference (ΔT_{end}) with absorption coefficient (a_s) is shown in Fig. 3 for 20 cities in Turkey (Table 2) and 4 different types of grounds given in Table 1. Calculations showed that, influence of the thermal conductivity of the ground on the results is insignificant. Therefore, only thermal diffusivity of the ground can be taken as characteristic physical property of the grounds.

The value of ground surface absorption coefficient (a_s) was varied between 0.6 to 0.9 in the calculations and all other parameters were kept constant. As can be seen from the figure, ΔT_{end} increases linearly with the increase of a_s.

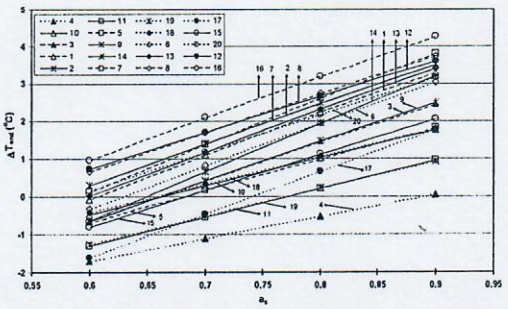


Fig. 3. Variation of temperature difference with absorption coefficient a_s for 20 cities (Table 2) in Turkey (f = 0.45).

Fig. 4 illustrates the variation of temperature difference (ΔT_{end}) with evaporation fraction (f) for 20 cities in Turkey (Table 2). It can be seen from the figure that ΔT_{end} decreases with the increase of f.

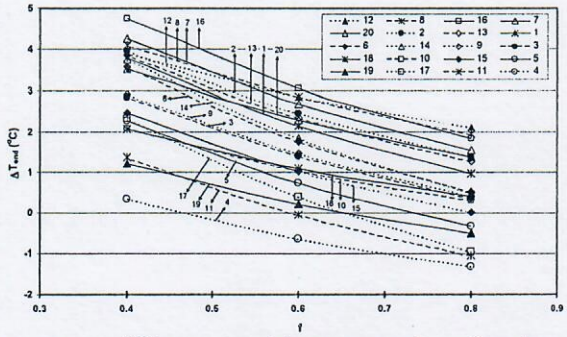


Fig. 4. Variation of temperature difference with evaporation fraction f for 20 cities (Table 2) in Turkey (a_s=0.9).

The temperature differences given in Figs. 3 and 4 can be expressed as follows:

$$\Delta T_{end} = A + B\,a_s + C\,f \tag{8}$$

A, B and C coefficients that were determined with statistical software are shown in Table 2. Since the difference between A coefficients for the cities considered is not significant, an arithmetic average value of -3.57 can be used.

$$A = -3.57 \tag{9}$$

Table 2. A, B and C coefficients for 20 cities in Eq. (8)

City Number	City	A	B	C
1	Adana	-3.64	11.26	-7.01
2	Afyon	-3.31	10.78	-6.35
3	Ankara	-3.98	10.28	-6.21
4	Antakya	-3.38	5.89	-4.12
5	Antalya	-2.83	8.44	-6.47
6	Aydın	-3.71	11.33	-7.56
7	Erzincan	-4.21	12.29	-6.71
8	Erzurum	-3.12	10.30	-5.31
9	Isparta	-4.19	10.58	-6.24
10	Istanbul	-3.00	7.53	-4.40
11	Izmir	-3.17	7.62	-6.01
12	Kars	-3.00	9.56	-4.42
13	Kayseri	-3.93	11.37	-6.37
14	Malatya	-4.71	12.87	-8.09
15	Mugla	-3.80	9.58	-6.10
16	Nigde	-2.40	11.06	-7.24
17	Sanliurfa	-4.74	11.37	-8.20
18	Tekirdag	-3.03	7.42	-4.11
19	Trabzon	-3.73	7.35	-4.30
20	Yozgat	-3.48	10.05	-5.29

The average value of daily mean values of solar radiation ($\dot{q}_{mean}$) for the whole year and mean ambient temperature (T_{mean}) for 20 years used in the calculations are given in Table 3.

B and C coefficients were determined as a function of $\dot{q}_{mean}$ and T_{mean}:

$$B = B_1 + B_2\,\dot{q}_{mean} + B_3\,T_{mean} \tag{10}$$

$$C = C_1 + C_2\,\dot{q}_{mean} + C_3\,T_{mean} \tag{11}$$

B_1, B_2, B_3 and C_1, C_2, C_3 coefficients were obtained using Statistica software from the B and C data given in Table 2 for different cities in Turkey. They are given in Table 4. In these cities $\dot{q}_{mean}$ and T_{mean} values are very different; $\dot{q}_{mean}$ varying between 129.6 W/m^2 and 221.35 W/m^2 and T_{mean} between 5.12 °C and 19.17 °C. Yearly mean temperatures and

insolation of different cities in USA and Europe are given in Table 5. One can see form the comparison of Tables 3 and 5 that the temperature and insolation values of the cities selected in this study cover also nearly all USA and Europe.

Table 3. $\dot{q}_{mean}$ and T_{mean} values used in the calculations for 20 cities

City	$\dot{q}_{mean}$ (W/m^2)	T_{mean} (^oC)
Adana	176.12	19.17
Afyon	182.54	11.30
Ankara	167.65	11.99
Antakya	152.78	18.33
Antalya	196.91	18.29
Aydın	189.66	17.76
Erzincan	172.62	11.02
Erzurum	184.57	5.14
Isparta	156.85	12.18
Istanbul	154.39	14.48
Izmir	187.22	18.02
Kars	171.80	5.12
Kayseri	169.64	10.61
Malatya	183.50	13.81
Mugla	168.23	15.06
Nigde	221.35	11.18
Sanliurfa	190.08	18.51
Tekirdag	146.48	13.96
Trabzon	129.62	14.01
Yozgat	165.04	9.04

Table 4. B_1, B_2, B_3, C_1, C_2, C_3 coefficients for 20 cities in Turkey

B_1	3.04
B_2	0.05
B_3	-0.12
C_1	2.72
C_2	-0.04
C_3	-0.08

Table 5. Yearly mean temperature and insolation for some cities in USA and Europe

City	$\dot{q}_{mean}$ (W/m^2)	T_{mean} (^oC)
Chicago (USA)	155	9.46
Houston (USA)	196	19.97
London (UK)	109	9.56
Munich (DE)	124	7.78
Paris (FR)	125	11.00
Bern (CH)	131	9.10
Athens (GR)	190	18.43

Temperature differences (ΔT_{end}) can be predicted by substituting the values of A, B and C coefficients which can be calculated from Eqs. 9-11, respectively. Comparison of numerically calculated and predicted (Eq. 8) values is shown in Fig. 5. It is seen from this figure that, the numerically calculated and predicted values compare satisfactorily.

Root Mean Square Error between numerically calculated and predicted values was found to be 0.58 °C.

3. 2. Relationship between ground end and maximum, minimum temperatures

The differences between the maximum (T_{max}) and the minimum (T_{min}) temperatures in the ground and ground end temperatures at 12 m depth (T_{end}) were determined. The following temperature differences were defined:

$$\Delta T_{max} = T_{max} - T_{end} \qquad (23\ January) \tag{12}$$

$$\Delta T_{min} = T_{end} - T_{min} \qquad (23\ July) \tag{13}$$

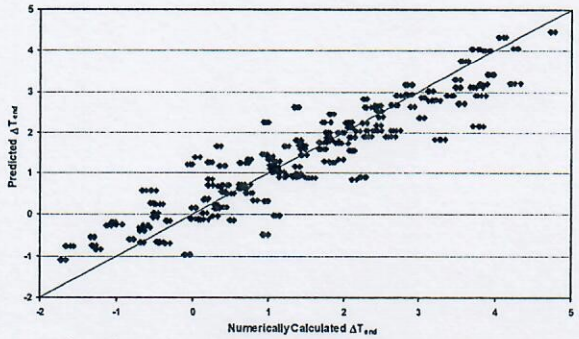


Fig. 5. Comparison of numerically calculated and predicted (Eq. 8) temperature differences.

Variation of maximum temperature difference (ΔT_{max}) with absorption coefficient (a_s) and evaporation fraction (f) is shown in Figs. 6 and 7, respectively. Figs. 8 and 9 demonstrate the variation of minimum temperature difference (ΔT_{min}) with absorption coefficient (a_s) and evaporation fraction (f) for 20 cities in Turkey, respectively. It is seen from Figs. 6, 7, 8 and 9 that dependency of ΔT_{max} and ΔT_{min} on the parameters a_s and f can be neglected. As a result, the following relationships can be written for T_{max} and T_{min}.

$$T_{max} = T_{end} + 0.48 \tag{14}$$

$$T_{min} = T_{end} - 0.48 \tag{15}$$

Root Mean Square Errors between the values calculated numerically and using the equations given above for T_{max} and T_{min} was found to be 0.06 °C for both.

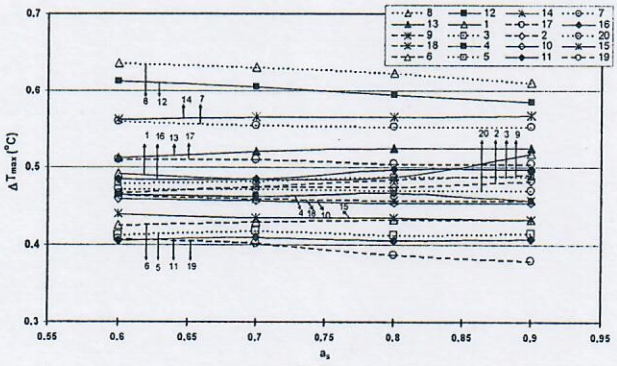


Fig. 6. Variation of maximum temperature difference with absorption coefficient a_s for 20 cities (Table 2) in Turkey (f = 0.45).

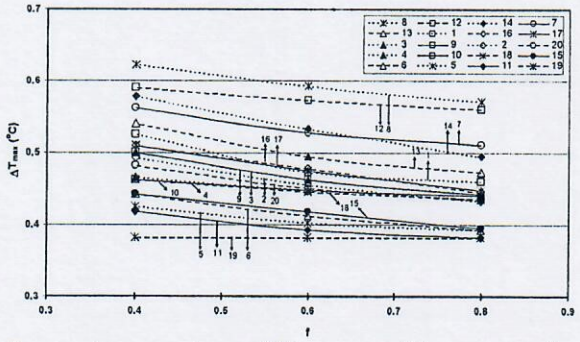


Fig. 7. Variation of maximum temperature difference with evaporation fraction f for 20 cities (Table 2) in Turkey (a_s = 0.9).

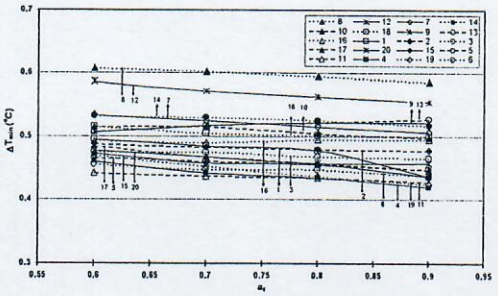


Fig. 8. Variation of minimum temperature difference with absorption coefficient a_s for 20 cities (Table 2) in Turkey (f = 0.45).

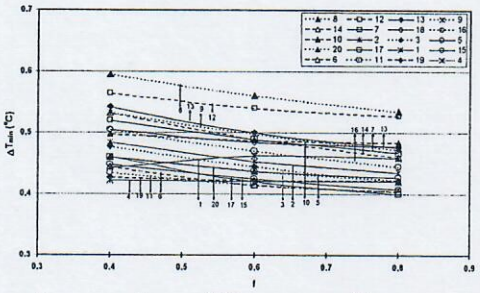


Fig. 9. Variation of minimum temperature difference with evaporation fraction f for 20 cities (Table 2) in Turkey (a_s=0.9).

3. 3. Relationship between ground physical properties and the depth of maximum and minimum temperatures

In this part of the study, the relationship between the ground physical properties and the depths at which maximum and minimum temperatures occur were investigated. Fig. 10 shows variation of the depths of maximum and minimum temperatures with thermal diffusivity (a) of various ground types.

In the calculations, while different thermal conductivity (k) values for one ground type were used, a value of the ground was kept constant. Results showed that, the depths of maximum and minimum temperatures do not change with k, they changes only with a value of the ground. The following equation was obtained for the depth L:

$$L = 2.44 + 5.43\ 10^{6}\ a \tag{16}$$

The depth L changes significantly with thermal diffusivity (a). While L is about 3 m for siliceous ground, it increases to approximately 8 m for granite. The other two ground types locate between these two limits.

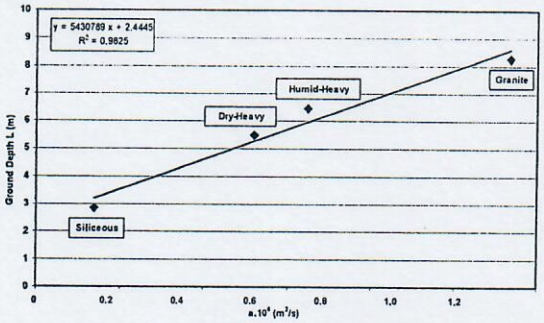


Fig. 10. Variation of the depths of maximum and minimum temperatures with thermal diffusivity of various ground types.

4. Conclusions

One layer ground temperatures for selected cities in Turkey were calculated and the depths for maximum and minimum ground temperatures and ground end temperatures were expressed in equations using the numerically obtained temperatures.

There is a relationship between temperature differences and yearly mean solar radiation ($\dot{q}_{mean}$) and yearly mean temperature (T_{mean}) for different ground types. In 23 January, the maximum temperature in the ground (T_{max}) can be taken 0.48 °C higher than the ground end temperature. In 23 July, the minimum temperature in the ground (T_{min}) can be taken 0.48 °C lower than the ground end temperature. The depths of maximum and minimum temperatures do not change with thermal conductivity of ground (k), it is only a function of thermal diffusivity (a) of the ground.

Acknowledgements

This study is supported by the Scientific and Technological Research Council of Turkey (TÜBİTAK) with the project number of 107M380.

Nomenclature

a	thermal diffusivity of ground [m²/s]
a_s	absorption coefficient of ground surface
f	evaporation fraction
h	heat transfer coefficient [W/m²K]
k	thermal conductivity of ground [W/mK]
L	ground depth [m]
L_{max}	ground depth of maximum temperature [m]
L_{min}	ground depth of minimum temperature [m]
p_{sa}	saturation pressure of water vapor at ambient temperature [Pa]
p_{ss}	saturation pressure of water vapor at ground surface temperature [Pa]
$\dot{q}$	solar radiation heat flux [W/m²]
$\dot{q}_{lw}$	long wave radiation heat flux [W/m²]
$\dot{q}_v$	heat flux due to the water vapor evaporation, [W/m²]
$\dot{q}_{mean}$	mean solar radiation heat flux [W/m²]
t	time [day]
T	temperature [°C]
T_a	ambient temperature [°C]
T_{end}	ground temperature at depth L [°C]
T_{max}	maximum temperature [°C]
T_{mean}	mean temperature [°C]
T_{min}	minimum temperature [°C]
T_s	ground surface temperature [°C]
u	wind speed [m/s]
x	soil depth [m]
φ	relative humidity

References

[1] El-Din MMS. On the heat flow in to the ground. Renew Energy 1999;18:473-490.
[2] Mihalakakou G, Santamouris M, Asimakopoulos DN. Modeling the earth temperature using multiyear measurements. Energy Build 1992;19:1-9.
[3] Mihalakakou G, Santamouris M, Lewis JO, Asimakopoulos DN. On the application of the energy balance equation to predict ground temperature profiles. Solar Energy 1997; 60:181-190.
[4] Mihalakakou G. On estimating soil surface temperature profile. Energy Build 2002;34:251-259.
[5] Nunes MN, Varas EA, Meza FJ. Modelling soil heat flux. Theor Appl Climatol 2010;100:251-260.
[6] Bilgili M. Prediction of soil temperature using regression and artificial neural network models. Meteorol Atmos Phys 2010;110:59-70.

[7] Droulia F, Lykoudis S, Tsiros I, Alvertos N, Akylas E, Garofalakis I. Ground temperature estimations using simplified analytical and semi-empirical approaches. Solar Energy 2009; 83:211-219.
[8] Tabari H, Sabziparvar AA, Ahmadi M. Comparison of artificial neural network and multivariate linear regression methods for estimation of daily soil temperature in an arid region. Meteorol Atmos Phys 2011;10:135–142.
[9] Gurel AE, Ergun A. Estimation of global solar radiation on horizontal surface using meteorological data. Energy Educ Sci Technol Part A 2012;28:941-948.
[10] Beltrami H. On the relationship between ground temperature histories and meteorological records: A report on the Pomquet station. Global Planetary Change 2001;29:327–348.
[11] Best MJ. A model to predict surface temperatures. Boundary-Layer Meteorology 1998; 88:279–306.
[12] Piechowski M. Heat and mass transfer model of a ground heat exchanger: Validation and sensitivity analysis. Int J Energy Res 1999; 23:571-588.
[13] Qin Z, Berliner P, Karnieli A. Numerical solution of a complete surface energy balance model for simulation of heat fluxes and surface temperature under bare soil environment. Appl Math Comput 2002;130:171–200.
[14] Rees SW, Zhou Z, Thomas HR. Ground heat transfer: A numerical simulation of a full-scale experiment. Build Environ 2007;42:1478–1488.
[15] Stathers RJ, Black TA, Novak MD, Bailey WG. Modeling surface energy fluxes and temperatures in dry and wet bare soils. Atmosph Ocean 1988;26-1:59-73.
[16] Yilmaz T, Ozbek A, Yılmaz A, Buyukalaca O. Influence of upper layer properties on the ground temperature distribution. J Thermal Sci Technol 2009;29:43-51.
[17] Yilmaz T, Buyukalaca O, Bulut H, Yilmaz A, Ozbek A. The Scientific and Technological Research Council of Turkey (TÜBİTAK) Final Report 2009; Project No:107M380.
[18] Dikmen E, Sencan A, Selbas R. Energetic and exergetic approach to vapor compression refrigeration cycle with two-stage and intercooler for new refrigerants. Energy Educ Sci Technol Part A 2011;26:205–219.
[19] Cerci Y, Okur M. The effects of reducing compressor suction inlet refrigerant vapor temperature on performance parameters for a household refrigerator. Energy Educ Sci Technol Part A 2011;28:105-116.
[20] Patrick EAF Soils. Longman, New York, 1983.
[21] Kizilkan O. Performance evaluation of variable speed refrigeration system with artificial neural networks. Energ Educ Sci Tech-A 2011;26:239–250.
[22] Orosa JA, García-Bustelo EJ. Permeable coverings as a sustainable solution for indoor air thermal comfort and energy saving. Energ Educ Sci Tech-A 2012;29:583-596.
[23] Ahamed JU, Saidur R, Masjuki HH, Sattar MA. Energy and thermodynamic performance of LPG as an alternative refrigerant to R-134a in a domestic refrigerator. Energ Educ Sci Tech-A 2012;29:597-610.
[24] Orosa JA. New methodology to define probability of buildings energy consumption. Energ Educ Sci Tech-A 2012;28:891–902.
[25] Orosa JA. A new validation tool of weather forecast for engineering applications. Energ Educ Sci Tech-A 2012;29:381-394.
[26] Orosa JA, Oliveira AC. A new understanding of building energy consumption. Energ Educ Sci Tech-A 2012;29:531-542.
[27] Orosa JA, García-Bustelo EJ. Permeable coverings as a sustainable solution for indoor air thermal comfort and energy saving. Energ Educ Sci Tech-A 2012;29:583-596.
[28] Orosa JA. New methodology to define probability of buildings energy consumption. Energ Educ Sci Tech-A 2012;28:891–902.